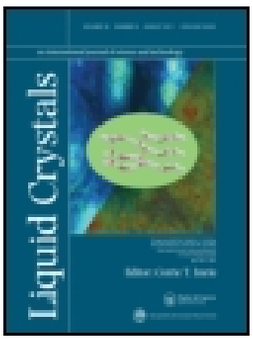

Liquid Crystals

ISSN: 0267-8292 (Print) 1366-5855 (Online) Journal homepage: http://www.tandfonline.com/loi/tlct20

Electrically tunable photo-aligned hybrid double-frequency liquid crystal polarisation grating

Song-zhen Li, Yong-gang Liu, Chun-Jie Liu, Zhi-Wei Zhao, Cheng-Miao Wang, Zeng-Hui Peng, Qi-dong Wang & Li Xuan

To cite this article: Song-zhen Li, Yong-gang Liu, Chun-Jie Liu, Zhi-Wei Zhao, Cheng-Miao Wang, Zeng-Hui Peng, Qi-dong Wang & Li Xuan (2018): Electrically tunable photo-aligned hybrid double-frequency liquid crystal polarisation grating, Liquid Crystals, DOI: 10.1080/02678292.2018.1485976

To link to this article: https://doi.org/10.1080/02678292.2018.1485976

Published online: 19 Jun 2018.

LIQUID CRYSTALS
https://doi.org/10.1080/02678292.2018.1485976

Taylor & Francis
Taylor & Francis Group

Electrically tunable photo-aligned hybrid double-frequency liquid crystal polarisation grating

Song-zhen Li[a,b], Yong-gang Liu[a], Chun-Jie Liu[a,b], Zhi-Wei Zhao[a,b], Cheng-Miao Wang[a,b], Zeng-Hui Peng[a], Qi-dong Wang[a] and Li Xuan[a]

[a]State Key Laboratory of Applied Optics, Changchun Institute of Optics, Fine Mechanics and Physics, Chinese Academy of Sciences, Changchun, China; [b]University of Chinese Academy of Sciences, Beijing, China

ABSTRACT

A polarisation grating (PG) based on the hybrid photo-aligned double-frequency liquid crystal has been demonstrated and fabricated in this paper. The single-order diffraction efficiency is above 95% for circular polarisation incident light. The PG can be driven by 2.5 V/μm electric field with alternating frequency and has no Freedericksz transition threshold. In response time, the rise time and decay time are 650 μs and 950 μs, respectively; the sub-millisecond can be achieved under a low driving voltage.

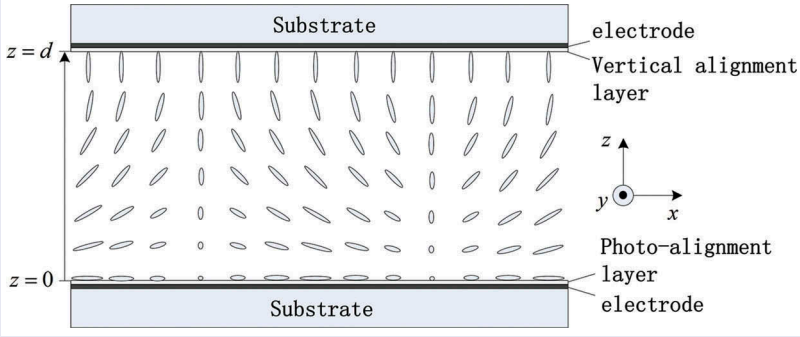

ARTICLE HISTORY
Received 5 April 2018
Accepted 4 June 2018

KEYWORDS
Polarisation grating; hybrid alignment; double-frequency liquid crystal; driving voltage; response time

1. Introduction

Liquid crystal (LC) is widely used in optical devices such as information display [1], spatial light modulator [2], beam shaping [3], laser beam steering and diffracted gratings [4–6] for the properties of optical anisotropy and electrically tenability. Recently, among the devices liquid crystal polarisation grating (LCPG) has attracted much attention [7]. The LCPG is thin, lightweight and can be fabricated easily. What's more, there are many excellent optical properties for LCPG such as perfect polarisation tenability, electro-optical tenability, large diffraction angles and extremely high single-order diffraction efficiency. So the LCPG is a promising element and has been applied in optical switch [8], laser beam steering [9], optical filters [10], polarisation imaging [11], displays [12] and so on. In structure, the LCPG features spatially varying, in-plane, linear birefringence. It employs the Pancharatnam–Berry phase principle and operates on circular eigen-polarisations [13–15]. Especially, it can diffract the incident light into the first orders with nearly 100% efficiency for circular polarisation incident light when cell thickness matches the half-wave phase retardation condition. LCPG was first realised by crowd in 2005 by polarisation holography with LC photo-alignment, but the diffraction efficiency is not high due to the LC molecules alignment default [15]. Then, with the development of fabrication technology, the diffraction efficiency is greatly improved approaching to 100% as described by theory. Subsequently the bandwidth of LCPG is improved to $\frac{\Delta\lambda}{\lambda} \sim 56\%$ by Oh with phase compensation [16]. Moreover operating voltage and response time are also important parameters for the performance of LCPG. For common nematic LCPG with cell thickness of 4 μm, the operating voltage is usually 20 V_{RMS}, and the response time is about tens of milliseconds that are mainly contributed by the time of LC molecules recovering to the initial state [17]. These disadvantages limit the application of LCPG. So LCPG with low operating voltage and fast response is in high demand. Hybrid-aligned nematic

CONTACT Qi-dong Wang qdwang@ciomp.ac.cn; Zeng-Hui Peng peng@ciomp.ac.cn

(HAN) cell structure is composed of two substrates with one substrate vertically aligned (VA) and the other parallelly aligned (PA). Due to the special structure HAN LC cell has no Freedericksz transition threshold and can works at a low operated voltage [18]. However, the phase retardation of HAN LC cell is only about the half of homogenous LC cell. To overcome this weakness, double-frequency liquid crystal (DFLC) is used. For the DFLC molecules, a low-frequency electric field makes them align perpendicularly to the substrates, but a high-frequency electric field makes them align parallelly to the substrates, so HAN cell can achieve the same phase retardation with homogenous cell for the same cell thickness. What's more, in both rise and decay processes, the electric field with alternating frequency drives the DFLC molecules to the equilibrium state; therefore, the LCPG with DFLC has the advantage of fast time response. All in all, the HAN cell LCPG with DFLC can work with low operating voltage and fast time response.

In this paper, we present the polarisation grating with HAN cell structure and DFLC material. This LCPG is fabricated with photo-alignment technology by polarisation holography. One of the substrates has spatially varying PA generated by polarisation holography photo-alignment technology, while the other is uniformly VA. We observe the far field diffraction of the HAN DFLC PG. Moreover, the electro-optical properties and response time are also measured. The HAN DFLC PG not only has extremely high single-order diffraction efficiency and polarisation tenability but also can work with low operating voltage and fast time response. Furthermore, HAN DFLC PG has no Freedericksz transition threshold.

2. Theory

Figure 1 illustrates the configuration of the HAN LCPG. The azimuthal angles of LC directors follow the equation: $\alpha(x) = \frac{\pi x}{\Lambda}$, where Λ is the optical grating period. The ideal diffraction efficiency at normal incidence can be derived with Jones matrix as follows [19]:

$$\eta_0 = \cos^2\left(\frac{\Gamma}{2}\right) \tag{1}$$

$$\eta_{\pm 1} = \frac{1 \mp S_3'}{2}\sin^2\left(\frac{\Gamma}{2}\right), \tag{2}$$

where η_m is the diffraction efficiency of the m diffraction order, and there are only three diffraction orders: $\pm$ 1st orders and 0th order, and S_3' is the normalised stokes parameter corresponding to the ellipticity of the incident light polarisation, for left and right circular polarisation, $S_3' = +1$ and -1 respectively. Γ is the birefringence phase retardation of the LC layer. It can be seen that the intensity distribution among the three orders depends on the polarisation of incident light and phase retardation of the LC cell. When the phase retardation Γ is chosen as half-wave retardation, all of the light will be diffracted to the 1st order, and if the incidence light is left or right circular polarisation all of the light will be diffracted to the −1st or +1st order, respectively.

In this patterned HAN cell, the initial tilt angle of LC could be obtained as $\theta_0(z) = \pi z/2d$, and d is the thickness of the LC cell. When an external electric field E is applied, the tilt angle of LC director can be given by [20]

$$\theta(z) = \theta_0(z) - \frac{\Delta\varepsilon E^2}{2k}\left(\frac{d}{\pi}\right)^2 \sin\left(\frac{\pi z}{d}\right) \tag{3}$$

The corresponding phase retardation Γ of LC layer can be expressed as

$$\Gamma = \frac{2\pi}{\lambda}\int_0^d \left(\frac{n_o n_e}{\sqrt{n_e^2\sin^2\theta(z) + n_o^2\cos^2\theta(z)}} - n_o\right)dz \tag{4}$$

where n_o and n_e are the ordinary and extraordinary refractive indices, respectively. Through applying an external electric voltage, we can modulate the intensity between the 1st order and 0th order. For a LC cell with appropriate thickness, the light can be totally diffracted

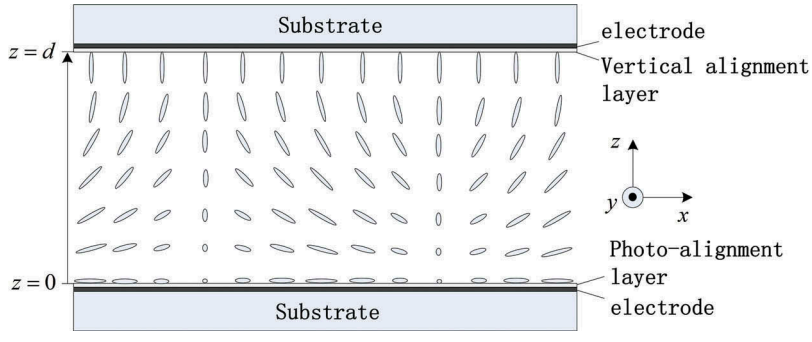

Figure 1. Schematic illustration of the HAN cell PG.

to the first orders. When a saturated high voltage is applied, LC molecules would be uniformly vertical alignment and all of the light would be diffracted to 0th order. Here, the saturated voltage is defined as one that the efficiency of the 0th order is up to 90%. For ordinary LCPG with homogenous cell, there is remarkable residual phase retardation even at a high driving voltage, because LC molecules may not be realigned due to surface anchoring. The residual phase retardation will lead to that the light of the 0th order leaks into the 1st orders. HAN cell structure can effectively reduce this effect. Figure 2 describes the curves of phase retardation versus voltages for the HAN cell and homogenous cell which is calculated according to the elastic continuum theory of the LCPG [21]. In the calculation, the wavelength is 633 nm and the frequency of voltage is 1 kHz; in addition, the parameters of material are the same as MO16 (from DIC, Dainippon Inks And Chemicals Incorporated). Obviously, the HAN cell has less residual phase retardation than the homogenous cell. Consequently, the LCPG with HAN cell has a lower driving voltage than the homogenous cell for the same extinction ratio. In this manner, an LCPG with a lower driving voltage and without decreasing the extinction ratio can be realised.

Besides the operation voltage, response time is also an important parameter for LCPG. The rise and decay times are defined as the duration time which the efficiency of the 0th order changes from 10% to 90% and from 90% to 10%, respectively. For common nematic LCs, the rise time of the LC cell can be greatly improved by applying a high voltage. However, the delay time that LC director recovers to the initial orientation is determined by the elastic and viscosity properties of the LC material.

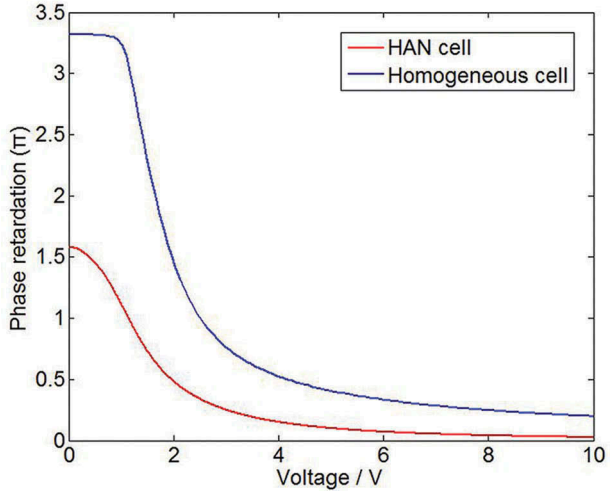

Figure 2. (Colour online) The phase retardation changes of two 4 μm cells in different alignments.

Therefore, the response time for the common nematic LCPG is limited to the level of tens of milliseconds. DFLC is a mixture that consists of LCs with opposite dielectric anisotropy [22,23]. It exhibits a positive dielectric anisotropy ($\Delta\varepsilon>0$) at a low-frequency ($f<f_c$) voltage, and turns to a negative dielectric anisotropy at a high-frequency voltage, where f_c is the crossover frequency. When a low-frequency ($f<f_c$) saturated voltage is applied, LC molecules tend to be VA, nearly all of incident light is diffracted into the 0th order. And when a high-frequency ($f>f_c$) saturated voltage is applied, LC molecules tend to be PA, and all of the light is diffracted into the 1st order for the PG with an appropriate cell thickness. In both the rise and delay processes, electric field is present to impel the LC molecules to the equilibrium state. So response time can be improved greatly with DFLC. What's more, the DFLC can overcome the shortcoming that the HAN cell has only the half-phase retardation related to the homogeneous cell. So the HAN DFLC PG has a fast response time relative to the ordinary LCPG. It would be very important for the application of PG in every field.

However, there is a challenge for DFLC devices. When applied with a high-frequency electric field, DFLC will absorb the electric field energy and generate heat, which in turn causes the crossover frequency drifting [24,25]. The DFLC with low crossover frequency would decrease the dielectric heating effect and reduce the electric field energy consumption for driving [26,27]. Therefore the DFLC MO16 (from DIC) with crossover frequency 8 kHz is chosen in this paper. In addition, DFLC is quite sensitive to the environmental temperature. Precisely controlled operation temperature can make them work well.

3. Experimental details

The method of the fabrication process of the LCPG in this paper is similar to that used by Oh and Escuti. It involves writing a polarisation holography into photo-alignment materials [28]. Polarisation holography records the polarisation distribution of the interference of two beams, rather than the intensity fringes. Two coherent beams with orthogonal circular polarisation are superimposed with a small angle, which creates a spatially varying linear polarisation distribution. Photo-alignment material makes LC molecules align following the linear polarisation distribution. The fabrication set-up is described schematically as Figure 3. The 325-nm laser is coupled into the hole by the micro-objective, and then collimated by lens. The collimated beam is divided into two beams with the same intensity by the BS. The two beams are reflected by mirrors and pass through the quarter-wave-plants which fast axes are perpendicular to each other

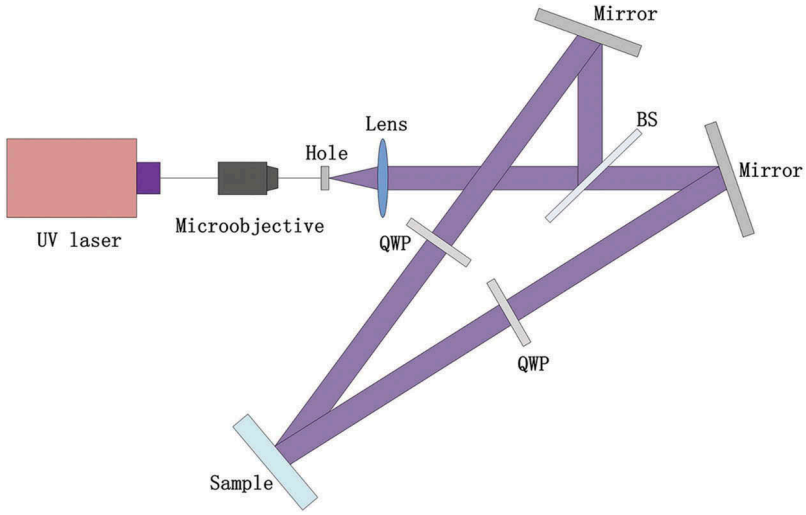

Figure 3. (Colour online) The schematic of the optical set-up for fabrication. BS: beam splitter; QWP: quarter-wave plate.

respectively, and are superimposed on the sample creating a spatially varying linear polarisation distribution.

The HAN cell consists of two indium-tin-oxide glass substrates. One of the indium-tin-oxide glass substrates is spin coated with vertical alignment layer, and the other is spin coated with photo-alignment layer. For the vertical alignment layer, we employ the polyimide (PI-5661, Nissan, Japan) layer. It makes the LC molecules align vertically along the surface of the substrate. For the photo-alignment layer, we use the photo-sensitive polymer called linear photo-polymerisable polymer (LPP, rolic-103) layer [29]. The two substrates are assembled together separated by 4-μm spacers. The measured cell gap is $4.0 \pm 0.1\mu m$. Then the assembled cell is exposed with orthogonal circular polarisation beams from HeCd (325 nm) laser and the dose of exposure is 5 J/cm^2. Next, the DFLC MO16 (from DIC) is infiltrated into the cell. The birefringence of MO16 is 0.235. So the cell with thickness 4 μm can meet the half-wave condition ($\Delta nd = \frac{3}{2}\lambda$) for wavelength 633 nm. Polarisation holograph establishes a spatially varying alignment condition in the LPP that follows the local linear polarisation direction distribution of the light. And the LC molecules align along the LPP profile to achieve the desired optical axis orientation. Now, the HAN DFLC PG is accomplished. As a contrast, we also fabricate a homogenous cell DFLC PG with the same cell thickness by the same way. All the fabrication process and experiment measures were done under the room temperature about 20°C.

4. Results and discussions

Figure 4 shows the micrographs of the HAN DFLC PG observed under a polarised optical microscope. The

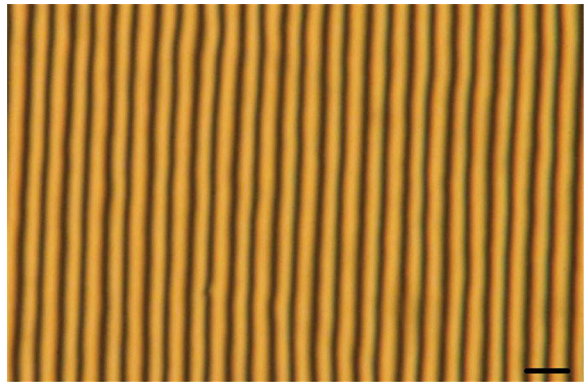

Figure 4. (Colour online) The micrograph of HAN DFLC PG observed under a polarised optical microscope. The scale bar in the figure is 25 μm.

space-variant directors of LC are exhibited by the continuous change of the brightness under the polarised optical microscope. For the regions that the LC directors are around 45° with respect to the polariser or analyser, we can see the bright domains, and for the regions that the LC directors are nearly parallel to the polariser or analyser, we can see the dark domains. Therefore, the bright-to-dark domains alternate twice along with the LC directors turning through π under the polarised optical microscope. When rotating the analyser, the bright and dark domains interconvert gradually, confirming the continuous varying of the director. This reveals that the designed director distribution is accurately transferred into the HAN cell. The far-field diffraction of the PG is verified by He-Ne laser (633 nm). When the linearly polarised light passes through the HAN PG and the high-frequency saturated voltage is applied, the diffracted pattern is captured by

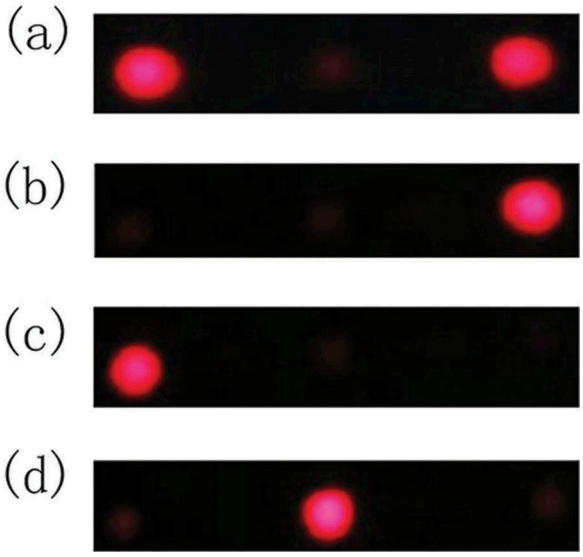

Figure 5. (Colour online) The far field diffraction of the HAN DFLC PG. (a) Diffraction pattern of linearly polarised incident light at high-frequency saturated voltage (20 kHz, 10 V_{RMS}). (b) Diffraction pattern of left circular polarised incident light at high-frequency saturated voltage. (c) Diffraction pattern of right circular polarised incident light at high frequency saturated voltage. (d) Diffraction pattern of HAN DFLC PG at low frequency saturated voltage (1 kHz, 10 V_{RMS}).

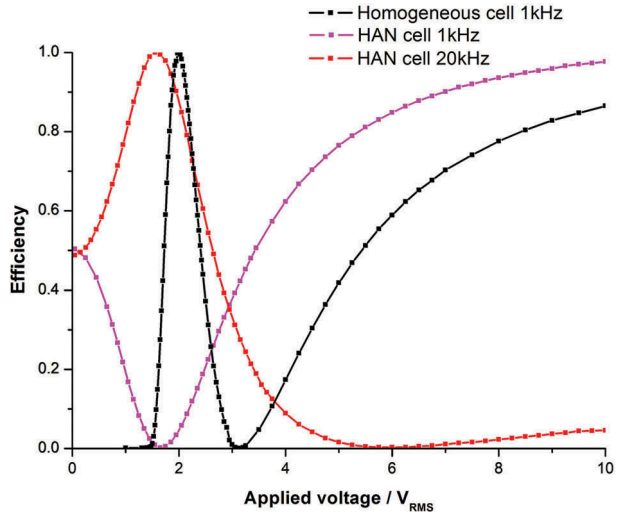

Figure 6. (Colour online) The voltage–efficiency curves of the HAN cell PG and homogeneous cell PG by measure. The spots are the data gotten by experimental measure, and the curves are formed by the connection of the spots.

the camera. As shown in Figure 5(a), there are only the 1st order and the 0th order is highly suppressed, indicating that the phase retardation matches the half-wave condition, and if the incident light is left circular polarisation, only the −1st order exists as shown in Figure 5 (b), for the right circular polarisation, there is only the +1st order as shown in Figure 5(c). For the circular polarisation incident light, the first-order diffraction efficiencies are both up to 95%. Figure 5(d) shows the far-field diffraction pattern of the HAN DFLC PG at the low-frequency saturated voltage, only the 0th order exists.

After that, the electro-optical properties of the HAN DFLC PG are measured. The voltage–efficiency curves are tested at first. Here, efficiency is defined as the intensity ratio of the objective order to the total transmitted light (ignoring the reflection loss, absorbing loss, scattering loss). In Figure 6, the red line and the pink line respect the voltage–efficiency curves of the 0th order of HAN cell DFLC PG while the black line respects the voltage–efficiency curve of the homogenous cell DFLC PG for circularly polarised incident light. Therein, the red and blue lines respect the voltage–efficiency curves of the HAN DFLC PG at frequencies of 1 and 20 kHz, respectively, and the black line respects the voltage–efficiency curve of homogeneous cell PG at the frequency of 1 kHz. It can be seen that for all the homogenous cell DFLC PG and the HAN DFLC PG with the low-frequency voltage of 1 kHz, the tilt angles of the LC directors gradually approach to 90° and the phase retardation Γ decreases gradually to zero with the increasing voltage, and the efficiency of the 0th order reaches the maximum. And for the HAN DFLC PG with the high-frequency voltage of 20 kHz, the tilt angles of the LC directors approaching to 0° and the phase retardation Γ increases gradually to maximum (the half-wave condition) with increasing voltage, so the efficiency of the 0th order reaches the minimum. Due to the cell gap is slightly larger than the optimised one, the 0th-order light which efficiency is below 2% exists. It can also be seen that the voltage of HAN cell PG gets saturated at 10 V_{RMS}; however, the voltage of homogenous cell PG requires a higher voltage. So the HAN cell PG can work at a lower operating voltage. Furthermore HAN cell PG has no Freedericksz transition threshold. These are the main advantages of HAN DFLC PG.

Then the response time of the HAN DFLC PG is also measured. In one hand, the rise time is measured with an applied low-frequency ($f = 1$kHz) saturated voltage, and in the other hand, the decay time is measured with an applied high-frequency ($f = 20$kHz) saturated voltage. As illustrated in Figure 7, a 10-V_{RMS} signal voltage is utilised with frequency alternating between 1 and 20 kHz, lasting for 5 ms each. In the meantime, the 0^{th}-order intensity converts between the minimum and maximum. However, the curve is not flat during the high-

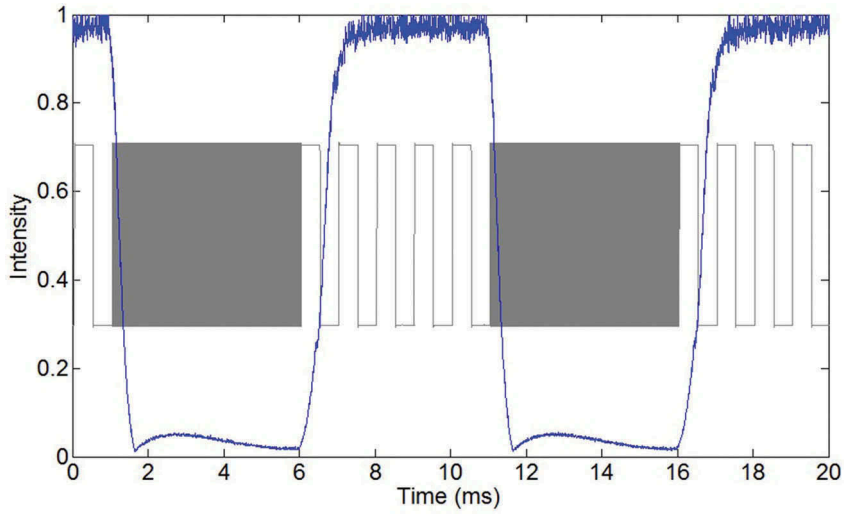

Figure 7. (Colour online) The response time of the HAN DFLC PG at the voltage of 10 V_{RMS}.

frequency addressing; we speculate that it is due to the flow effect, the phenomenon could be suppressed by optimising the viscoelastic coefficient of DFLC material. According to Figure 7, the rise time and the decay time are 650 and 950 μs, respectively. The HAN DFLC PG can achieve the sub-millisecond scale response time at a low operating voltage. And the response time can be further improved by increasing the applied voltage or decreasing the cell thickness.

5. Conclusion

In this paper, we proposed and demonstrated the LCPG with HAN cell structure and DFLC material. This HAN DFLC PG is realised by polarisation holography. The HAN DFLC PG has extremely high single-order diffraction efficiency over 95% and polarisation tenability. Moreover, the HAN DFLC PG can operate at a low electric field of ~2.5V_{RMS}/μm and with no Freedericksz transition threshold. The rise and decay time are 650 and 950 μs, respectively, when the HAN DFLC PG is driven with alternating-frequency saturated voltage. The operating voltage and response time can be further improved by decreasing the cell thickness. The PG described as above has high single-order diffraction efficiency and can work at a low electric field but has a sub-millisecond scale response time. These excellent properties will make LCPG be widely used in display, photonics and so on.

Acknowledgements

The authors are indebted to Rolic Company for their kind support with the photo-alignment material. This work was sponsored by the National Natural Science Foundation of China (11604327, 11174274, 11174279, 61205021 and 11204299) and the Science Foundation of State Key Laboratory of Applied Optics.

Disclosure statement

No potential conflict of interest was reported by the authors.

Funding

This work was supported by the National Natural Science Foundation of China [11604327, 11174274, 11174279, 61205021, 11204299] and Science Foundation of State Key Laboratory of Applied Optics.

References

[1] Chen HW, Lee JH, Lin BY, et al. Liquid crystal display and organic light-emitting diode display: present status and future perspectives. Light Sci Appl. 2018;7:17168.
[2] Zhang Z, You Z, Chu D. Fundamentals of phase-only liquid crystal on silicon (LCOS) devices. Light Sci Appl. 2014;3:e213.
[3] Chen P, Lu YQ, Hu W. Beam shaping via photopatterned liquid crystals. Liq Cryst. 2016;43:2051–2061.
[4] Avci N, Hwang SJ. Electrically tunable polarisation-independent blue-phase liquid crystal binary phase grating via phase-separated composite films. Liq Cryst. 2017;44:1–7.
[5] Li H, Wang C, Pan Y, et al. Transient holographic grating in azo-dye-doped liquid crystals with off-resonant light. Liq Cryst. 2016;44:1–6.
[6] Chien CY, Sheu CR. Small dosage of holographic exposure via a He-Ne laser to fabricate tunable liquid crystal phase gratings operated with low electric voltages. Liq Cryst. 2016;44:1–9.

[7] Tervo J, Turunen J. Paraxial-domain diffractive elements with 100% efficiency based on polarization gratings. Opt Lett. 2000;25:785.
[8] Serak SV, Hakobyan RS, Nersisyan SR, et al. All-optical diffractive/transmissive switch based on coupled cycloidal diffractive waveplates. Opt Exp. 2012;20:5460–5469.
[9] Kim J, Oh C, Serati S, et al. Wide-angle, nonmechanical beam steering with high throughput utilizing polarization gratings. Appl Opt. 2011;50:2636–2639.
[10] Nicolescu E, Escuti MJ. Polarization-independent tunable optical filters using bilayer polarization grating. Appl Opt. 2010;49:3900–3904.
[11] Kudenov MW, Escuti MJ, Dereniak EL, et al. White-light channeled imaging polarimeter using broadband polarization gratings. Appl Opt. 2011;50:2283.
[12] Chen H, Weng Y, Xu D, et al. Beam steering for virtual/augmented reality displays with a cycloidal diffractive waveplate. Opt Exp. 2016;24:7287.
[13] Pancharatnam S. Generalised theory of interference and its applications. Proc Indian Acad Sci. 1957;46:1–18.
[14] Berry MV. Quantal phase factors accompanying adiabatic changes. Proc R Soc Lond Ser A. 1984;392:45–57.
[15] Eakin JN, Xie Y, Pelcovits RA, et al. Zero voltage Freedericksz transition in periodically aligned liquid crystals. Appl Phys Lett. 2004;85:1671–1673.
[16] Oh C, Escuti MJ. Achromatic diffraction from polarization gratings with high efficiency. Opt Lett. 2008;33:2287–2289.
[17] Wei BY, Chen P, Ge SJ, et al. Fast-response and high-efficiency optical switch based on dual-frequency liquid crystal polarization grating. Opt Mater Exp. 2016;6:597–602.
[18] Lu YQ, Liang X, Wu YH, et al. Dual-frequency addressed hybrid-aligned nematic liquid crystal. Appl Phys Lett. 2004;85:3354–3356.
[19] Provenzano C, Pagliusi P, Cipparrone G. Highly efficient liquid crystal based diffraction grating induced by polarization holograms at the aligning surfaces. Appl Phys Lett. 2006;89:2588.
[20] Lin XW, Hu W, Hu XK, et al. Fast response dual-frequency liquid crystal switch with photo-patterned alignments. Opt Lett. 2012;37:3627.
[21] Komanduri RK, Escuti MJ. Elastic continuum analysis of the liquid crystal polarization grating. Phys Rev E. 2007;76:021701.
[22] Schadt M. Low-frequency dielectric relaxations in nematics and dual-frequency addressing of field effects. Mol Cryst Liq Cryst. 2006;89:77–92.
[23] Xianyu H, Wu S, Lin C. Dual frequency liquid crystals: a review. Liq Cryst. 2009;36:717–726.
[24] Wen CH, Wu ST. Dielectric heating effects of dual-frequency liquid crystals. Appl Phys Lett. 2005;86:186.
[25] Lee YCHW. Lower operation voltage in dual-frequency cholesteric liquid crystals based on the thermodielectric effect. Opt Expess. 2013;21:23927–23933.
[26] Song Q, Xianyu H, Gauza S, et al. High birefringence and low crossover frequency dual-frequency liquid crystals. Mol Cryst Liq Cryst. 2008;488:179–189.
[27] Xianyu H, Liang X, Sun J, et al. High performance dual frequency liquid crystal compounds and mixture for operation at elevated temperature. Liq Cryst. 2010;37:1493–1499.
[28] Crawford GP, Eakin JN, Radcliffe MD, et al. Liquid-crystal diffraction gratings using polarization holography alignment techniques. J Appl Phys. 2005;98:1671.
[29] Schadt M, Schmitt K, Kozinkov V, et al. Surface-induced parallel alignment of liquid crystals by linearly polymerized photopolymers. Jpn J Appl Phys. 1992;31:2155–2164.